A Bilevel Approach to Operational Decision Making of a Distribution Company in Competitive Environments

Hossein Haghighat, *Member, IEEE*, and Scott W. Kennedy, *Member, IEEE*

***Abstract*—This paper presents a model for operational decision making of a distribution company (disco) with distributed generation (DG) and interruptible loads (IL) in a competitive market. The disco objective, modeled through the upper-level problem, is to minimize the cost of market purchases and DG unit dispatch while taking into account the responses of the other discos. This upper-level problem is constrained by a lower-level market clearing problem whose objective corresponds to maximization of social welfare. Such a setting results in a multi-disco equilibrium problem formulated as an equilibrium problem with equilibrium constraints (EPEC) by combining the optimality conditions of all upper-level problems. Using a nonlinear approach, the EPEC problem is reformulated as a single nonlinear optimization model which is simultaneously solved for all discos. The proposed approach is applied to an ac model of a power system to account for voltage and reactive power constraints of the transmission and distribution networks. Numerical examples based on two test systems are presented to illustrate the application of the proposed method.**

***Index Terms*—Distributed generation (DG), equilibrium problem with equilibrium constraints (EPEC), interruptible load (IL).**

NOMENCLATURE

A. Sets and Indices

i, j	Indices for transmission system nodes.
n	Index for distribution system nodes.
u	Index for generating units.
v	Index for discos.
N_v	Set of distribution nodes of disco v.
R	Set of transmission nodes.
H	Set of discos.
J_i	Set of generating units placed at node i.
F	Set of transmission lines.
M	Set of distribution feeders.

B. Parameters

$P_{L,i}, Q_{L,i}$	Real and reactive load at transmission node i.
$P_{L,v,n}, Q_{L,v,n}$	Real and reactive load at distribution node n of disco v.
$a_{Pg,u,i}, b_{Pg,u,i}$	Parameters of real power cost function of generator u at node i.
$a_{Qg,u,i}, b_{Qg,u,i}$	Parameters of reactive power cost function of generator u at node i.
$a_{dg,v,n}, b_{dg,v,n}$	Parameters of real power cost function of the DG unit at node n of disco v.
$a_{IL,v}, b_{IL,v}$	Parameters of cost function of aggregate interruptible load of disco v.
$a_{IL,v,n}, b_{IL,v,n}$	Parameters of cost function of interruptible load at node n of disco v.
$pf_{IL,v}$	Power factor of interruptible load of disco v.
$R_{P,u,i}, R_{Q,u,i}$	Real and reactive revenue of generator u at node i.
$R_{P,v,n}$	Real power revenue of the DG unit at node n of disco v.

C. Variables

$P_{g,u,i}, Q_{g,u,i}$	Real and reactive power of generator u at node i.
$P_{dg,v,n}, Q_{dg,v,n}$	Real and reactive power of the DG unit at node n of disco v.
$P_{IL,v,n}, Q_{IL,v,n}$	Real and reactive power of IL at node n of disco v.
$P_{IL,v}, Q_{IL,v}$	Real and reactive power of the aggregate IL of disco v.
$P_{s,v}, Q_{s,v}$	Real and reactive power imported by disco v.
P_i, Q_i	Real and reactive power injections at transmission node i.
$P_{v,n}, Q_{v,n}$	Real and reactive power injections at node n of disco v.

Manuscript received May 07, 2011; revised September 08, 2011 and November 15, 2011; accepted December 21, 2011. Date of publication April 05, 2012; date of current version October 17, 2012. Paper no. TPWRS-00420-2011.

H. Haghighat is with the Department of Electrical Engineering, University of Jahrom, Jahrom, Iran (e-mail: haghighat@jia.ac.ir).

S. Kennedy is with the Masdar Institute of Science and Technology, Abu Dhabi, UAE (e-mail: skennedy@masdar.ac.ae).

Digital Object Identifier 10.1109/TPWRS.2011.2182214

V_i	Voltage magnitude of transmission node i.
$V_{v,n}$	Voltage magnitude of distribution node n of disco v.
e, f	Real and imaginary coordinates of transmission bus voltage.
e_v, f_v	Real and imaginary coordinates of distribution bus voltage of disco v.
$L^P_{v,s,i}, L^Q_{v,s,i}$	Active and reactive power losses of the substation transformer of disco v.
$\hat{S}_{nk,v}$	Average apparent flow of feeder between node n and k of disco v.
$\hat{S}_{ij}$	Average apparent flow of transmission line between node i and j.

D. Symbols

$(^-)$, $(\_)$, $(\hat{})$	Upper, lower, and average values of (.).
$a \perp b$	Complementarity conditions between a and b.
$a \circ b$	Entry-wise matrix product of a and b.

I. Introduction

THE main role of a distribution company (disco) is to serve customer loads at satisfactory voltage magnitudes and feeder loading levels. A disco has to develop a rational operating strategy with regards to dispatching distributed generation (DG) units, interrupting customer loads, and purchasing power from the wholesale market while maintaining system security. In many instances discos play the role of retailers that buy power at volatile prices on the wholesale market and resell it at fixed tariffs to small customers. Discos and retailers are generally separate market entities with differences in purposes, networks, and sizes [1], [2]. Nevertheless, from an operational perspective they share very similar problem formulations whose objectives are cost minimization while satisfying physical, financial and regulatory constraints. Such a disco-retailer with the responsibility of network operation is considered in [3] and a two-stage hierarchical model for determining the operational decisions on grid purchases, scheduling of DG, and interruptible load is developed. A model for energy acquisition of a disco with DG and interruptible load (IL) are proposed in [4] based on the ac optimal power flow (OPF) model. Reference [5] proposes a market integration mechanism for DG in a pool-based system which encompasses both energy and capacity payment procedures in the wholesale market with DG units located at distribution level.

Equilibrium models have been used for modeling the competition between market participants. Such an approach is presented in [6] wherein a multi-period energy acquisition model is developed for a disco with DG and IL options in a day-ahead market. Using a bilevel optimization method, the competition between discos is modeled as an equilibrium problem with equilibrium constraints (EPEC) and solved using a nonlinear complementarity method (NCM). EPECs arise in the analysis of multi-leader-follower games where multiple dominant firms compete non-cooperatively [7]. The Stackelberg game is the simplest form of a multi-leader-follower game in which there is only one leader and multiple followers who react to the leader's strategy. The Stackelberg game can be formulated as a mathematical program with equilibrium constraints (MPEC). Reference [8] presents a noninterior point method for solving a Stackelberg game in an ac model of a power system. Diagonalization techniques based on the Gauss-Seidel or Gauss-Jacobi methods have been used as well for solving EPECs. They solve a cyclic sequence of MPEC problems until the decision variables of all leaders reach a fixed point [9], [10]. Leyferr and Munson construct a multi-leader-follower game and present the nonlinear complementarity problem (NCP) and NLP formulations of the EPEC [11]. In the NCP approach, each MPEC problem is replaced by its strong stationarity conditions and the equivalent KKT conditions for all leaders are combined to form an EPEC model while in the NLP formulation the complimentarity constraints are penalized and moved into the objective to yield a well-defined NLP problem. Bautista *et al.* apply the NLP and NCP approaches to formulate a multi-leader single-follower game in an ac power flow model [12], [13]. An NCP approach is developed in [14] for solving a multi-firm equilibrium problem using a dc transmission model and a nonlinear complementarity function for reformulating the NCP problem as a set of nonlinear algebraic equations. A bilevel approach is proposed in [14] for solving the optimal contract price problem of a DG unit in a distribution system.

In a competitive environment, the interaction between discos and the impacts of rival responses should be taken into account in the operational decision making of a disco. While equilibrium properties of multi-generator game problems have been investigated in the technical literature, very few studies focus on the competition at the distribution side, with the possible exception of [6]. In [6], the interaction between discos is studied using a linear dc OPF program and a simplified disco model wherein DG units and ILs are placed at the transmission level. Simplified disco models cannot capture the impact of DG units and ILs on the feeder losses, voltage profiles, and power flow of the distribution system. Moreover, although dc power flow models can account for the thermal limits of transmission lines, they cannot directly consider voltage and reactive power constraints which have similar congestion effects as real power and are deemed essential for establishing correct nodal prices of real and reactive power. Ensuring that reactive power is correctly priced is especially important to create an appropriate basis for efficient consumption of reactive power and a non-discriminatory basis for suppliers' compensation. To accurately account for these issues, the entire transmission and distribution networks should be modeled based on ac OPF methods.

In view of the above discussion, the main objectives and contributions of this paper are:

1) To develop an operational decision making model for a disco in a competitive environment with DG units and IL options. The proposed model considers a full ac model of the distribution network and its interconnection with the

transmission grid. In the so developed model DG units and interruptible loads are located at the distribution level and their impacts on feeder losses, voltage profiles, and power flow of the distribution system are accurately accounted for.

2) The competition between discos is considered using a bilevel optimization method. The disco objective, modeled through the upper-level problem, is to minimize the cost of market purchases and DG units dispatch while taking into account the responses of other discos. This upper-level problem is constrained by a lower-level market clearing problem whose objective corresponds to social welfare maximization. The upper- and lower-level problems are formulated based on security-constrained ac-OPF models.
3) The discos operational decision making problem is thus formulated as a multi-disco EPEC model and solved using the NLP approach proposed in [11]. In this approach, the lower-level problem of all individual discos is substituted by its equivalent KKT conditions and the strong stationarity conditions of all discos are combined to produce a set of nonlinear equations which can be solved by standard NLP solvers. Different techniques including a nonlinear MPEC formulation as well as two ex-post heuristic methodologies are proposed to verify the optimal characteristics of the equilibrium point.

The rest of the paper is organized as follows. Section II describes market assumptions and introduces the bilevel mathematical model. The NLP formulation of the bilevel model and the diagonalization technique are also presented in Section II. Section III presents and discusses the numerical results of two test systems. The computational issues of the optimization models and the characteristics of the solution and formulations are discussed in Section IV. Concluding remarks are provided in Section V.

II. Mathematical Formulation

A. Market Assumptions

A pool-based market composed of the ISO, discos and gencos is considered. The ISO operates the market through the security-constrained ac OPF. Offers from generators for real and reactive power supply and offers from discos for load interruption, together with the information on the maximum and minimum real and reactive power output of generators are submitted to the ISO. The cost function of real power generation is given by $C(P_{g,u,i}) = a_{Pg,u,i}P^2_{g,u,i} + b_{Pg,u,i}P_{g,u,i}$. The operational cost of reactive power is approximated by $C(Q_{g,u,i}) = a_{Qg,u,i}Q^2_{g,u,i} + b_{Qg}Q_{g,u,i}$, assuming it reflects the cost of MW-losses arising from reactive power generation or absorption in the main and auxiliary parts of the power plant [16], [17]. To avoid binary variables in the model, the fixed cost component is omitted assuming this cost is absorbed in the bid curve of the generator. Given that rate designs for reactive power largely vary among power markets and no uniform structure has yet evolved, in this work we assume that reactive suppliers are eligible for receiving payments for reactive power supply. This payment is intended to cover the operational cost of the supplier for reactive power provision. Moreover, we assume that this payment is calculated based on the nodal price of reactive power at the transmission level. Discos connected to the transmission grid are also charged for reactive power consumption based on the nodal price. The major benefit of nodal pricing is that all providers are paid or charged on a non-discriminatory basis, as per FERC recommendation [18]–[21].

We assume that the disco is also the retailer which owns and operates the distribution network (see [28] and [29] for realistic market structures wherein a disco-retailer participates as a player at the distribution level). The disco interacts with the wholesale market and the other discos, and is connected to the transmission grid via a substation transformer. The disco has multiple operational options including dispatching DG units, offering IL to the market, and wholesale market purchases. We assume that DG units are owned and operated by the disco. The IL offered by the disco, at the interconnection point with the transmission system, is an aggregate amount equal to the sum of individual ILs inside the distribution network. The cost function of the aggregate IL is approximated by $C(P_{IL,v}) = a_{IL,v}P^2_{IL,v} + b_{IL,v}P_{IL,v}$ [2], [5], [6], where coefficients $a_{IL,v}$, $b_{IL,v}$ are equal to the average of the coefficients of the individual cost functions of ILs in the distribution network. We assume that the disco will transfer the ISO payment for load interruption to its customers and collect no profit.

The cost function of real power production of DG units is given by $C(P_{dg,v,n}) = a_{dg,v,n}P^2_{dg,v,n} + b_{dg,v,n}P_{dg,v,n}$. In this work, we do not consider an explicit cost model for reactive power of DG units mainly because the cost depends on the DG technology [22] which is not considered in this work. Analogous to the transmission system, the payment to DG units for real power generation is calculated at the nodal prices of the distribution system. Nodal pricing can yield larger revenues for DG resources and reward them for reducing feeder losses [23], [24]. The application of nodal pricing in distribution systems is discussed in [15] and [25].

It is assumed that discos can estimate the cost information of the other participants, and are aware of the market clearing process; hence, they will take the ISO problem as part of the constraints in their own problems.

B. Bilevel Model

The decision making problem pertaining to a disco that develops an optimal operating strategy by minimizing its operating cost can be formulated as a bilevel optimization problem. The upper-level problem represents the decisions to be made by the disco with regard to dispatching DG units, market purchases, and offering IL to the market while maintaining distribution system security. The lower-level problem represents the market clearing mechanism performed by the ISO seeking to minimize the cost of real and reactive power production as well as load interruption subject to system security.

The disco's operational decision making problem can be thus formulated as the following bilevel model. The dual variables are provided after the corresponding constraints separated by colon:

$$\text{Minimize} \quad f_v = \sum_{n\in N_v} \left\{a_{dg,v,n}{P_{dg,v,n}}^2 + b_{dg,v,n}P_{dg,v,n}\right\} + \{\lambda_{P,i}P_{s,v} + \lambda_{Q,i}Q_{s,v}\} \tag{1}$$

subject to

$$P_{s,v} - L^P_{v,s}(\mathbf{e},\mathbf{f},\mathbf{e}_v,\mathbf{f}_v) + P_{dg,v,n} + P_{IL,v,n} - P_{L,v,n} - P_{v,n}(\mathbf{e}_v,\mathbf{f}_v) = 0 : \rho_{P,v,n} \quad \forall n \in N_v \tag{2}$$

$$Q_{s,v} - L^Q_{v,s}(\mathbf{e},\mathbf{f},\mathbf{e}_v,\mathbf{f}_v) + Q_{dg,v,n} + c_{pf,v,n}P_{IL,v,n} - Q_{L,v,n} - Q_{v,n}(\mathbf{e}_v,\mathbf{f}_v) = 0 : \rho_{Q,v,n} \quad \forall n \in N_v \tag{3}$$

$$\underline{V}^2_{v,n} \le V^2_{v,n}(\mathbf{e}_v,\mathbf{f}_v) \le \bar{V}^2_{v,n} : \bar{\mu}_{V,v,n},\ \underline{\mu}_{V,v,n} \ \forall n \in N_v \tag{4}$$

$$\underline{P}_{dg,v,n} \le P_{dg,v,n} \le \bar{P}_{dg,v,n} : \bar{\mu}_{Pdg,v,n},\ \underline{\mu}_{Pdg,v,n} \ \forall n \in N_v \tag{5}$$

$$\underline{Q}_{dg,v,n} \le Q_{dg,v,n} \le \bar{Q}_{dg,v,n} : \bar{\mu}_{Qdg,v,n},\ \underline{\mu}_{Qdg,v,n} \ \forall n \in N_v \tag{6}$$

$$\underline{P}_{s,v} \le P_{s,v,i} \le \bar{P}_{s,v} : \bar{\mu}_{Ps,v},\ \underline{\mu}_{Ps,v} \tag{7}$$

$$\underline{Q}_{s,v} \le Q_{s,v,i} \le \bar{Q}_{s,v} : \bar{\mu}_{Qs,v},\ \underline{\mu}_{Qs,v} \tag{8}$$

$$\hat{S}_{nk,v}(\mathbf{e}_v,\mathbf{f}_v)^2 \le {\bar{S}_{nk,v}}^2 : \mu_{nk,v} \quad \forall n,k \in M \tag{9}$$

$$\underline{P}_{IL,v,n} \le P_{IL,v,n} \le \bar{P}_{IL,v,n} : \bar{\mu}_{IL,v,n}\ \underline{\mu}_{IL,v,n} \forall n \in N_v \tag{10}$$

$$P_{IL,v} = \sum_{n\in N_v} P_{IL,v,n} \quad : \rho_{IL,v} \tag{11}$$

$$\text{Minimize} \ f_{ISO} = \sum_{i\in R, u\in J_i} \Big\{a_{Pg,u,i}{P_{g,u,i}}^2 + b_{Pg,u,i}P_{g,u,i} + a_{Qg,u,i}{Q_{g,u,i}}^2 + b_{Qg,u,i}Q_{g,u,i}\Big\} + \sum_{v\in H} a_{IL,v}{P_{IL,v}}^2 + b_{IL,v}P_{IL,v} \tag{12}$$

subject to

$$\sum_{u\in J_i} P_{g,u,i} - P_{L,i} - (P_{s,v} - P_{IL,v}) - P_i(\mathbf{e},\mathbf{f}) = 0 : \lambda_{P,i} \quad \forall i \in R \tag{13}$$

$$\sum_{u\in J_i} Q_{g,u,i} - Q_{L,i} - (Q_{s,v} - c_{pf,v}P_{IL,v}) - Q_i(\mathbf{e},\mathbf{f}) = 0 \quad : \lambda_{Q,i} \forall i \in R \tag{14}$$

$$\hat{S}_{ij}(\mathbf{e},\mathbf{f})^2 \le \bar{S}^2_{ij} \quad : \pi_{ij} \quad \forall i,j \in F \tag{15}$$

$$\underline{V_i}^2 \le V_i^2(\mathbf{e},\mathbf{f}) \le \overline{V_i}^2 \quad : \bar{\pi}_{V,i},\ \underline{\pi}_{V,i} \quad \forall i \in R \tag{16}$$

$$\underline{P}_{g,u,i} \le P_{g,u,i} \le \bar{P}_{g,u,i} \quad : \bar{\pi}_{Pg,u,i},\ \underline{\pi}_{Pg,u,i} \quad \forall u \in J_i \tag{17}$$

$$\underline{Q}_{g,u,i} \le Q_{g,u,i} \le \bar{Q}_{g,u,i} \quad : \bar{\pi}_{Qg,u,i},\ \underline{\pi}_{Qg,u,i} \quad \forall u \in J_i \tag{18}$$

$$\underline{P}_{IL,v} \le P_{IL,v} \le \bar{P}_{IL,v} \quad : \bar{\pi}_{IL,v},\ \underline{\pi}_{IL,v} \quad \forall v \in H \tag{19}$$

$$Q_{IL,v} = c_{pf,v}P_{IL,v}, \quad c_{pf,v} \triangleq \tan\left(\cos^{-1}\left(pf_{IL,v}\right)\right) \quad \forall v \in H. \tag{20}$$

Model (1)–(20) comprises the upper-level problem (1)–(11) and the lower-level problem (12)–(20). The upper-level problem represents the disco's operating strategy while the lower-level problem solves for the aggregated power produced and interrupted load at each transmission level node and the corresponding nodal prices. Note that $\lambda_{P,i}$, $\lambda_{Q,i}$ in (1) are nodal prices of real and reactive power at the interconnection point with the transmission system calculated as the dual variables of power balance constraints (13) and (14), respectively.

The objective function in (1) represents the cost of power supplied by DG units, the cost of real and reactive power purchased from the market at the nodal prices of the transmission system. The constraints in (2)–(3) enforce the real and reactive power balance at every distribution level node. The loss components $L^P_{v,s,i}$ and $L^Q_{v,s,i}$ account for the losses in the substation transformer subtracted from the power imported by the disco. Note that e_v and f_v in (2)–(3) denote real and imaginary components of bus voltage in a rectangular coordinate (see Appendix A or [12] for details on rectangular coordinate). Constraint (4) enforces upper and lower bounds on the voltage magnitude of the distribution system nodes. Constraints (5) and (6) state that the real and reactive power produced by DG units should be within limits. Constraints (7) and (8) imply the power imported to the distribution system should not exceed the substation transformer capacity. Constraint (9) enforces the MVA-flow limits on distribution feeders. Note that in (9) we use the average flow of apparent power calculated from real and reactive flows on both feeder directions [12]. Constraint (10) imposes upper and lower bounds on the power interrupted at each distribution node. Constraint (11) states that the aggregate IL, offered to the market, is the sum of individual ILs inside the distribution system.

The objective function (12) of the lower-problem is the cost of real and reactive power generation and the cost of remuneration for load interruption. Constraints (13)–(14) are the power balance equations for real and reactive power at the transmission level, respectively. The MVA-flow limits on transmission lines are expressed by (15) where, similar to (9), the average flow in both directions is used. The voltage limits of the transmission system are represented by (16). Constraints (17)–(18) impose upper and lower bounds on the power produced by the generators. Constraint (19) enforces upper and lower limits on load interruption at the disco interconnection point. Finally, constraint (20) states that reactive power is interrupted at a constant power factor.

C. NLP Formulation

To derive the NLP formulation, the KKT conditions of the lower-level problem (12)–(19) are obtained and incorporated in the upper-level problem. For simplicity of derivation, let us write the above equations in a general form and discard subscripts. The KKT conditions of the lower-level problem (12)–(20) can be written as

$$\nabla_{\mathbf{y}_1} f_{ISO}(\mathbf{y}_1) - \lambda_P \nabla_{\mathbf{y}_1} h_{IP}(\mathbf{y}_1) - \lambda_Q \nabla_{\mathbf{y}_1} h_{IQ}(\mathbf{y}_1) - \boldsymbol{\pi}\nabla_{\mathbf{y}_1} h_I(\mathbf{y}_1) = 0 \tag{21}$$

$$h_{IP}(\mathbf{y}_1) = 0 \tag{22}$$

$$h_{IQ}(\mathbf{y}_1) = 0 \tag{23}$$

$$0 \le \boldsymbol{\pi} \perp h_I(\mathbf{y}_1) \ge 0 \tag{24}$$

where h_{IP} and h_{IQ} denote the real and reactive power equality constraints and h_I stands for the inequality constraints of the lower-level problem. The set of control and state variables of the lower-level problem including e_i, f_i, $P_{g,u,i}$, $Q_{g,u,i}$, and $P_{IL,v,i}$ is abbreviated by $\mathbf{y}_1$. The dual variables associated with constraints (15)–(19) are denoted by $\boldsymbol{\pi}$. In order to compactly write

(21)–(24), let us define (25) at the bottom of the page, where $\mathbf{y} = (\mathbf{y}_1, \boldsymbol{\pi}, \boldsymbol{\lambda})$ and $\boldsymbol{\lambda} = (\lambda_P, \lambda_Q)$. After introducing slack variables $\mathbf{s}$ in h_I, the nonlinear complementarity model (21)–(25) can be written in the following form:

$$h_E(\mathbf{y}) = 0 \tag{26}$$
$$h_I(\mathbf{y}_1) - \mathbf{s} = 0 \tag{27}$$
$$0 \le \mathbf{s} \perp \boldsymbol{\pi} \ge 0. \tag{28}$$

Given the above observations and that the complementarity conditions $0 \le \mathrm{a} \perp \mathrm{b} \ge 0$ can be formulated in the nonlinear form $\mathrm{a} \ge 0$, $\mathrm{b} \ge 0$, $-\mathrm{ab} \ge 0$, the disco's optimal operating strategy problem can be expressed as the following nonlinear problem:

$$\text{Minimize} \quad f_v(\mathbf{x}_v, \boldsymbol{\lambda}) \tag{29}$$
subject to
$$h_{DE,v}(\mathbf{x}_v, \mathbf{y}_1) = 0 \quad : \rho_v \tag{30}$$
$$h_{DI,v}(\mathbf{x}_v) \ge 0 \quad : \mu_v \tag{31}$$
$$h_E(\mathbf{y}) = 0 \quad : \phi_{E,v} \tag{32}$$
$$h_I(\mathbf{y}_1) - \mathbf{s} = 0 \quad : \phi_{I,v} \tag{33}$$
$$\mathbf{s} \ge 0 \quad : \varphi_{1,v} \tag{34}$$
$$\boldsymbol{\pi} \ge 0 \quad : \varphi_{2,v} \tag{35}$$
$$-\boldsymbol{\pi} \circ \mathbf{s} \ge 0 \quad : \varphi_{3,v} \tag{36}$$

where $h_{DE,v}$ and $h_{DI,v}$ stand for the equality and inequality constraints of the upper-level problem. The vector of the disco variables including $e_{v,n}$, $f_{v,n}$, $\mathbf{P}_{dg,v,n}$, $\mathbf{Q}_{dg,v,n}$, $\mathbf{P}_{IL,n,v}$, $\mathbf{P}_{s,v,i}$, and $Q_{s,v,i}$ is abbreviated by $\mathbf{x}_v$. These variables are outputs of the upper-level problem while $\mathbf{y}$ denotes the decision variables of the ISO in the lower-level problem. Disco problems share the ISO variables which are inputs to the upper-level problems. The decision variable of discos other than disco $\boldsymbol{v}$ is denoted by $\mathbf{x}_{-v}$. The vector of the dual variables associated with the equality constraints of the upper-level problem is denoted by $\boldsymbol{\rho}_v = (\rho_{P,v}, \rho_{Q,v}, \rho_{IL,v})$. Observe that each disco assigns a different set of dual variables to common KKT conditions (32)–(36). Applying strong stationarity [11] to problem (29)–(36) yields the following nonlinear complementarity formulation:

$$\nabla_{x_v} f_v - \rho_v \nabla_{x_v} h_{DE,v} - \mu_v \nabla_{x_v} h_{DI,v} - \phi_{E,v} \nabla_{x_v} h_E = 0 \tag{37}$$
$$\rho_v \nabla_{y_1} h_{DE,v} + \phi_{E,v} \nabla_{y_1} h_E + \phi_{I,v} \nabla_{\mathbf{y}_1} h_I = 0 \tag{38}$$
$$\nabla_{\boldsymbol{\lambda}} f_v - \phi_{E,v} \nabla_{\boldsymbol{\lambda}} h_E = 0 \tag{39}$$
$$\phi_{E,v} \nabla_{\boldsymbol{\pi}} h_E + \varphi_{2,v} - \varphi_{3,v} \circ \mathbf{s} = 0 \tag{40}$$
$$\phi_{I,v} - \varphi_{1,v} + \boldsymbol{\pi} \circ \varphi_{3,v} = 0 \tag{41}$$
$$h_{DE,v} = 0 \tag{42}$$
$$h_E = 0 \tag{43}$$
$$h_I - \mathbf{s} = 0 \tag{44}$$
$$0 \le \mu_v \quad \perp \quad h_{DI,v} \ge 0 \tag{45}$$
$$0 \le \varphi_{1,v} \quad \perp \quad \mathbf{s} \ge 0 \tag{46}$$
$$0 \le \varphi_{2,v} \quad \perp \quad \boldsymbol{\pi} \ge 0 \tag{47}$$
$$0 \le \varphi_{3,v} \quad \perp \quad -\boldsymbol{\pi} \circ \mathbf{s} \ge 0. \tag{48}$$

Considering that (46)–(48) can be expressed in the equivalent form below:

$$0 \le \varphi_{1,v} \perp \mathbf{s} \ge 0 \tag{49}$$
$$0 \le \varphi_{2,v} \perp \boldsymbol{\pi} \ge 0 \tag{50}$$
$$0 \le \boldsymbol{\pi} \perp \mathbf{s} \ge 0 \tag{51}$$
$$\varphi_{3,v} \ge 0. \tag{52}$$

By introducing slack variables $\mathbf{z}_v$ to $h_{DI,v} \ge 0$, the complementarity constraint (45) can be written as

$$0 = h_{DI,v} - \mathbf{z}_v \tag{53}$$
$$0 \le \mu_v \perp \mathbf{z}_v \ge 0. \tag{54}$$

The NLP formulation of problem (29)–(30) is derived by replacing the complementarity constraints in problem (37)–(54) by the equivalent nonlinear form. Since there are multiple discos in the market, the complete NLP formulation of the multi-disco equilibrium problem is thus obtained by combining the strong stationarity conditions for each disco as described in the following:

$$\text{Minimize} \quad C_{pen} = \sum_{v \in H} \{\varphi_{1,v}\mathbf{s} + \varphi_{2,v}\boldsymbol{\pi} + \mu_v \mathbf{z}_v\} + \boldsymbol{\pi}\mathbf{s} \tag{55}$$
subject to
$$\nabla_{\mathbf{x}_v} f_v - \rho_v \nabla_{\mathbf{x}_v} h_{DE,v} - \mu_v \nabla_{\mathbf{x}_v} h_{DI,v} - \phi_{E,v} \nabla_{\mathbf{x}_v} h_E = 0 \quad \forall\, v \in H \tag{56}$$
$$\rho_v \nabla_{\mathbf{y}_1} h_{DE,v} + \phi_{E,v} \nabla_{\mathbf{y}_1} h_E + \phi_{I,v} \nabla_{\mathbf{y}_1} h_I = 0 \;\forall\, v \in H \tag{57}$$
$$\nabla_{\boldsymbol{\lambda}} f_v - \phi_{E,v} \nabla_{\boldsymbol{\lambda}} h_E = 0 \quad \forall\, v \in H \tag{58}$$
$$\phi_{E,v} \nabla_{\boldsymbol{\pi}_\mathbf{y}} h_E + \varphi_{2,v} - \varphi_{3,v} \circ \mathbf{s} = 0 \quad \forall\, v \in H \tag{59}$$
$$\phi_{I,v} - \varphi_{1,v} + \boldsymbol{\pi} \circ \varphi_{3,v} = 0 \quad \forall\, v \in H \tag{60}$$
$$h_{DE,v} = 0 \quad \forall\, v \in H \tag{61}$$
$$h_{DI,v} - \mathbf{z}_\mathbf{v} = 0 \quad \forall\, v \in H \tag{62}$$
$$h_E = 0 \tag{63}$$
$$h_I - \mathbf{s} = 0 \tag{64}$$
$$\mu_v \ge 0 \quad \forall\, v \in H \tag{65}$$
$$\mathbf{z}_v \ge 0 \quad \forall\, v \in H \tag{66}$$
$$\varphi_{1,v} \ge 0 \quad \forall\, v \in H \tag{67}$$

$$0 = h_E(\mathbf{y}) = \begin{pmatrix} \nabla_{\mathbf{y}_1} f_{ISO}(\mathbf{y}_1) - \lambda_P \nabla_{\mathbf{y}_1} h_{IP}(\mathbf{y}_1) - \lambda_Q \nabla_{\mathbf{y}_1} h_{IQ}(\mathbf{y}_1) - \boldsymbol{\pi} \nabla_{\mathbf{y}_1} h_I(\mathbf{y}_1) \\ h_{IP}(\mathbf{y}_1) \\ h_{IQ}(\mathbf{y}_1) \end{pmatrix} \tag{25}$$

$$\varphi_{2,v} \geq 0, \quad \forall\, v \in H \tag{68}$$
$$\varphi_{3,v} \geq 0, \quad \forall\, v \in H \tag{69}$$
$$\boldsymbol{\pi} \geq 0 \tag{70}$$
$$\mathbf{s} \geq 0. \tag{71}$$

Note that complementarity conditions are moved into the objective by a penalty parameter of one. In this formulation, discos share the KKT conditions of the lower-level problem. These constraints link the disco problems with each other producing an EPEC model. Note that lower-level problem is nonconvex and hence, the KKT conditions are not sufficient for guaranteeing the optimality of the solution. The NLP formulation (55)–(71) aims to provide a feasible solution by leading complementarity conditions to zero while enforcing all the original system constraints. Since the equilibrium conditions are nonconvex, any solution set $(\mathbf{x}_v{}^*, \mathbf{y}^*, \mathbf{s}^*, \mathbf{z}_v{}^*, \boldsymbol{\rho}_v{}^*, \boldsymbol{\mu}_v{}^*, \boldsymbol{\varphi}_{\mathbf{E},v}{}^*, \boldsymbol{\Phi}_{I,v}{}^*, \boldsymbol{\Psi}_1{}^*, \boldsymbol{\Psi}_2{}^*, \boldsymbol{\Psi}_3{}^*)$ with $C_{pen} = 0$ has to be tested to ensure it corresponds to a local minimum (see also [12]). In this work, three different approaches are proposed to verify the optimality of the solution. In the first approach we use an alternative MPEC formulation of the multi-disco EPEC problem and the diagonalization method for solving it. This solution approach has been successfully applied to EPEC problems in electricity markets (see [9], [10], [26], [27]). The diagonalization method implements an iterative procedure for solving a sequence of MPEC problems until an equilibrium point is found. We implement the diagonalization technique based on the nonlinear Gauss-Seidel method, which performs the following steps:

1) *Initialization*: Assuming a starting point and a convergence tolerance ε, set the current iteration step k to be 0.
2) *Loop over MPEC problems*: Solve the nonlinear MPEC problem (29)–(36) at each iteration k while fixing the decision variables of the rest discos, $\mathbf{x}_{-v}$ at the most recently available information. Denote the solution as $X_v^{(k)} = (\mathbf{x}_v^{(k)}, \mathbf{y}^{(k)})$.
3) *Check convergence*: Repeat step 2) until the accuracy tolerance, $\Delta_{tol} = \Sigma_v \| X_v^{(k+1)} - X_v^{(k)} \| \leq \varepsilon$, is satisfied or, the maximum number of iterations is reached.

The outcomes of the MPEC problem can be compared to the outcomes of the EPEC model. As a simple test, if these results match, up to the numerical accuracy of the solver, it is a strong indicator that an optimal equilibrium is achieved. Otherwise, the stationary point may correspond to a local maximum or a saddle point. In addition to the above test, which is based on an alternative problem formulation, we will implement two ex-post heuristic tests to examine the characteristics of the solution. These tests are described in Section IV.

III. Test System Results

The optimization results of two test systems are presented in this section. The first test system, referred to as Test system A, is composed of three networks including two distribution networks and a single ISO grid. The second test system, referred to as Test system B, corresponds to a larger system where the IEEE 30-bus system is used as the ISO grid and 5 distribution systems, used in Test system A, represent discos. A number of scenarios are created to illustrate the application of the proposed method.

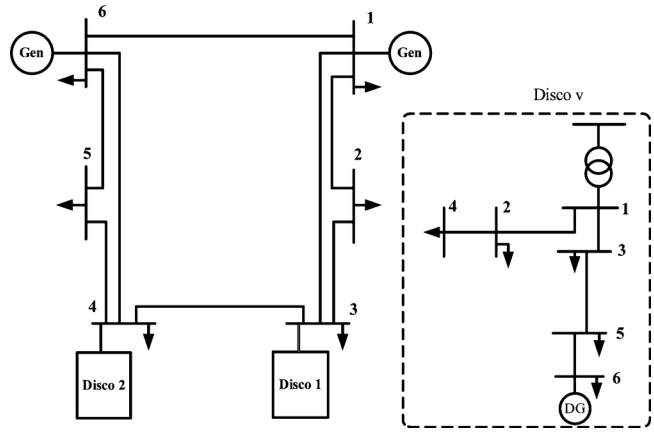

Fig. 1. Test system A: The ISO grid and distribution systems.

A. Test System A

Test system A consists of the ISO grid and two disco networks as shown in Fig. 1. The ISO grid is composed of six buses, eight branches, two generators, and inelastic demands at buses. The base load of the ISO grid is 34.2 MW and 22 Mvar. Two similar distribution networks are connected to the ISO grid at buses 3 and 4 via substation transformers as shown in Fig. 1. Each distribution system has a radial configuration with six buses, five feeders, and one DG unit at the remote-end bus 6. The capacity of each substation transformer is 10 MVA. The data of the ISO and distribution networks are presented in Appendix B. The maximum amount of real power that can be interrupted at each distribution node is set to 25% of the demand. A constant power factor of 0.95 is applied to all load buses for reactive power curtailment.

Four different cases are studied as described next. Case 1 represents the base case scenario. In case 2, the load in the ISO grid increases by 10% while the load in each disco increases by 20%. In case 3 none of the discos are allowed to offer IL to the market. Case 4 maintains the conditions in case 3 and further assumes that the capacity of the DG units in both distribution systems is reduced by 50%.

Note that DG output levels and market purchases are the main outputs of the upper level problem while the main input to the lower-level problems is the IL offers from discos. The optimization results of the ISO and disco systems are presented in Tables I and II. In Table I, the average nodal prices, real and reactive power produced, the load interrupted and the revenue of generators are shown. It is seen that the output levels of generators and the average nodal price slightly increase in cases 2–4 mainly because operational constraints become binding. Note that the generator at node 6 is always fully dispatched because it is cheaper. Table I also shows that in case 1 and case 2, the IL offered by both discos are called for because the ISO can reduce costs by means of load interruption. It is seen that in case 3 and case 4 the generators' revenues significantly increase because

TABLE I
OPTIMIZATION RESULTS OF THE ISO GRID—TEST SYSTEM A

Index	*Suffix*	*Case 1*	*Case2*	*Case 3*	*Case 4*
λ_P^{avg} ($/MWh)	–	104.65	104.74	104.85	105.04
λ_Q^{avg} ($/Mvarh)	–	3.40	3.45	3.47	3.47
P_g (MW)	1,1	0.11	2.37	4.35	8.39
	1,6	30.0	30.0	30.0	30.0
Q_g (Mvar)	1,1	1.40	3.56	3.83	3.63
	1,6	12.01	14.10	14.49	14.03
P_{IL} (MW)	1	2.11	2.53	0.0	0.0
	2	2.12	2.55	0.0	0.0
R_P ($)	1,1	11.5	249.4	457.4	881.5
	1,6	3113.9	3117.4	3120.5	3127.0

TABLE II
OPTIMIZATION RESULTS OF DISCOS—TEST SYSTEM A

Index	*v*	*Case 1*	*Case2*	*Case 3*	*Case 4*
ρ_P^{avg} ($/MWh)	1	28.63	29.34	29.80	105.02
	2	28.83	29.59	30.40	104.71
ρ_Q^{avg} ($/Mvarh)	1	2.68	2.88	2.95	4.00
	2	2.57	2.79	2.87	3.92
P_{dg} (MW)	1	7.260	8.78	9.62	7.5
	2	7.58	9.17	10.0	7.5
P_s (MW)	1	0	0	0	1.85
	2	0	0	0	2.18
Q_s (Mvar)	1	1.96	3.17	3.63	3.53
	2	2.93	4.22	4.72	4.17
MW-losses	1	0.42	0.57	0.68	0.40
	2	0.45	0.63	0.75	0.43
IL profit ($)	1	24.3	29.3	0	0
	2	30.7	37.1	0	0
Operating cost ($)	1	188.7	231.4	254.5	396.1
	2	199.5	244.2	266.7	431.3

the ISO sells more power to discos. Note that in case 4 generators' revenues are maximized since discos purchase higher amounts of power to meet their demand.

Table II presents the optimization results for disco 1 and disco 2. It is seen that the (average) nodal prices of real and reactive power increase in cases 2–4. This is expected because in these cases either the distribution load increases or stronger constraints are imposed on ILs and/or DG units. Note that when the IL option becomes unavailable in case 3 and case 4, DG units run at full capacity because they are cheaper than the wholesale power. The reactive output level of DG units is not shown in Table II because it is fixed at 3.33 Mvar which is capacity limit of DG units. Note that the cost of reactive power of DG units is assumed to be negligible and thus, discos utilize the full capacity of these units to reduce the cost. It is to be mentioned that DG units are required to operate at a fixed power factor for security reasons. To include the effect of such constraints, we instead assume that DG units have limited reactive power capability. It is seen in Table II that discos have to purchase reactive power from the ISO market in every case due to insufficient reactive supply in the distribution systems while they need to import real power only in the last case.

The MW-losses of the distribution systems are also shown in Table II. The highest losses take place in case 3 where the whole system load is met by a remotely located DG unit which in turn increases the feeder losses. Note that losses in case 4 are nearly identical with the losses in the base case because the disco can supply part of the system load from the ISO grid, via the substation transformer, which is located at a shorter distance to loads (i.e., nodes 2 and 4 of the distribution systems in Fig. 1). Compared to the base case, the IL profit increases in case 2 because a larger amount of power, at a higher price, is interrupted. Finally, the last row of Table II shows the operating costs of the discos. The highest operating cost is associated with case 4 where discos have to import real power at the wholesale price, which is more expensive than the power supplied by the DG units. Note that the minimum operating cost of discos takes place in the base case wherein DG units and IL are available for providing operational flexibility in the decision making process of the discos.

B. Test System B

In this test system, the IEEE 30-bus system represents the ISO grid and five distribution systems, described in Test system A, represent the discos. To differentiate between discos, they are divided into two groups based on their information. Discos residing in each group have similar information in terms of DG capacity, IL data, and system load. Discos 1, 3, and 5 form the first group and disco 2 and disco 4 make up the second group.

The IEEE 30-bus test system is composed of 30 buses and 41 branches with a base load of 283.4 MW and 126.2 Mvar. We use a modified IEEE 30-bus system with six generators. Discos 1–5 are connected to buses 14, 16, 19, 21, and 24, respectively.

Four cases are studied as described next. Case 1 represents the base case scenario. In case 2, the first group of discos increases the cost of IL by 50% while all other conditions remain as in the base case. In case 3, the load in discos 1, 3, and 5 increases by 25% and the other conditions are maintained as in case 2. Case 4 is built based on case 3 wherein the cost of IL in discos 2 and 4 increases by 50% and the load in the ISO grid increases by 17%. The rest conditions in case 4 are identical with case 3.

The optimization results of the ISO system are summarized in Table III. Compared to the base case, the average nodal prices and system losses increase in cases 2–4 because either the system load increases or a smaller amount of load is interrupted. It is seen from Table III that in comparison with the base case the load interrupted in case 2 and case 3 decreases by 6.4 MW due to the increase in the IL cost. Note that in these two cases the ISO invokes no IL from the first group of discos and interrupts 4.9 MW from the second group (i.e., discos 2 and 4). In case 4, although the second group raises the cost of IL by 50%, the ISO needs to interrupt nearly 0.6 MW of load because all generators reach their limits. Thus, to meet the system load in case 4, the ISO chooses the cheapest IL offered by disco 5 (see Table IV). Note that transmission losses are minimized in the base case although the ISO's load is identical with the load in case 2 and case 3. This illustrates the role of IL in reducing losses.

The load payment shown in Table III is calculated using the nodal prices of real power. Moreover, payments associated with the real and reactive power imports of the discos are determined based on the nodal prices at the interconnection with the ISO grid. Notice the large payments of loads and discos in case 4 due to increase in nodal prices. Notice that we assume that only

TABLE III
OPTIMIZATION RESULTS OF THE ISO SYSTEM —TEST SYSTEM B

Index	*Case 1*	*Case2*	*Case 3*	*Case 4*
λ_P^{avg} ($/MWh)	50.4	50.6	50.8	91.3
λ_Q^{avg} ($/Mvarh)	2.3	2.4	2.5	5.4
IL (MW)	11.3	4.9	4.9	0.6
MW-losses	4.2	4.3	4.4	7.5
Mvar-losses	20.9	22.2	23.2	37.1
MW produced	282.0	288.4	294.3	355.0
Mvar produced	131.8	138.6	143.4	190.0
IL revenue ($)	568	254	255	53
MW-revenue ($)	13782	14131	14451	30835
Mvar-revenue ($)	214	226	239	501
Load payment ($)	14312	14352	14390	30148
Disco payment ($)	317	326	628	1673

TABLE IV
OPTIMIZATION RESULTS OF DISCOS —TEST SYSTEM B

Index	*v*	*Case 1*	*Case2*	*Case 3*	*Case 4*
ρ_P^{avg} ($/MWh)	1	27	28	51	91
	2	53	53	54	104
	3	27	28	51	90
	4	52	52	53	101
	5	27	28	52	42
P_{IL} (MW)	1	2.11	0.00	0.00	0.00
	2	2.47	2.47	2.47	0.00
	3	2.11	0.00	0.00	0.00
	4	2.47	2.47	2.47	0.00
	5	2.11	0.00	0.00	0.58
P_{dg} (MW)	1	7.19	9.54	10.00	10.00
	2	8.75	8.75	8.75	8.75
	3	7.19	9.54	10.00	10.00
	4	8.75	8.75	8.75	8.75
	5	7.21	9.57	10.00	10.00
P_s (MW)	1	0.00	0.00	1.91	1.97
	2	2.85	2.85	2.86	5.66
	3	0.00	0.00	1.90	1.97
	4	2.83	2.83	2.84	5.60
	5	0.00	0.00	1.93	1.34
Q_s (Mvar)	1	0.87	1.86	3.14	3.23
	2	3.36	3.36	3.43	5.59
	3	0.87	1.86	3.14	3.22
	4	3.34	3.34	3.35	5.01
	5	0.89	1.89	3.18	2.96
Losses (MW)	1	0.35	0.59	0.72	0.79
	2	0.65	0.65	0.66	1.00
	3	0.35	0.59	0.72	0.79
	4	0.65	0.65	0.66	0.94
	5	0.65	0.65	0.65	0.88
Operating cost ($)	1	182	243	353	444
	2	376	377	379	804
	3	182	243	353	442
	4	373	374	375	780
	5	182	244	357	391

discos are charged for reactive power consumption. Moreover, the ISO payment to generators for reactive power supply is computed based on the nodal price of this service at the generator node. This payment is intended to cover the operational cost of reactive power supply, as previously explained. It can be seen from Table III that in every case the ISO collects merchandising surplus.

The optimization results of the discos are shown in Table IV. From Table IV it is seen that the optimization results for discos in the same group are very close. The average nodal price of real power, shown in Table IV, remains approximately constant for disco 2 and disco 4 through cases 1–3 while for the rest of the discos it nearly doubles in case 3 as the load increases in the first group of discos and DG units reach output limits. Compared to the base case, nodal prices substantially increase in case 4 because IL offers are not accepted except for disco 5 which curtails 0.6 MW of load to meet the ISO need. Similar observations hold for the reactive power price not shown in Table IV.

As explained earlier, the maximum amount of IL is accepted in the base case since they are comparable with the cost of power produced by generators. The output levels of DG units in MW are also shown in Table IV. It is seen that DG units in discos 2 and 4 (i.e., the second group of discos) always operate at their limits (note that the capacity of DG units belonging to the first group is 25% higher than that of the second group). As the load increases in the distribution systems, DG units hit output limits in cases 3 and 4. The reactive output levels of DG units are not shown in Table IV because they are fixed at 3.33 Mvar.

From Table IV it is seen that discos 2 and 4 needs to purchase real power from the ISO in the first and second cases while they have to import real power in cases 3 and 4 due to load increase in the distribution systems. Notice the differences in the outcomes of reactive power. All discos have to rely on the ISO grid for reactive power through all the cases including the base case. It is seen that the imports of real and reactive power to discos are maximum in case 4 because the load in the distribution systems increases. In this case, only disco 5 curtails 0.6 MW of power to meet the ISO need. Losses in the distribution systems are also presented in Table IV. It is seen that MW losses increase in cases 2–4. Similar conclusions can be drawn for Mvar losses. Finally, the operating costs of the discos are shown in Table IV. As expected, the operating cost will increase as the system load increases. Note that market purchases constitute a significant portion of the operating cost of discos because they are charged at market prices, which are much higher than the cost of power produced by DG units. For instance, in case 4 market prices of real and reactive power are approximately 92 $/MWh and 6 $/Mvarh, respectively, while the production cost of real power of DG units is nearly 30 $/MWh and the cost of reactive power is negligible. Thus, the disco has to pay 30 $ higher for every MW or Mvar it purchases from the ISO.

IV. COMPUTATIONAL ISSUES

A. Solution Characterization of the MPEC and EPEC Models

The optimization results presented in Section IV were obtained by solving the NLP problem (55)–(71). As previously indicated, the optimization results need to be verified to ensure optimality. In this section, we check the optimal property of the results by solving the MPEC problem (29)–(36) using the procedure outlined in Section II. We will compare the outcomes of this MPEC model with the solution of the EPEC problem. If these results match, this provides strong evidence that an optimal equilibrium is achieved. In the following subsections the characteristics of the solution are further examined using ex-post approaches.

In the case of Test system A, the solution found by the NLP approach was exactly the same as the solution of the diagonalization method. Table V compares the problem size and the

TABLE V
COMPARISON OF OPTIMIZATION MODELS—TEST SYSTEM A

Index	NLP method	Diagonalization method
Number of variables per problem	605	113
Number of constraints per problem	377	117
Total CPU seconds	24.0	2.5
Total solver iterations	975	399
Accuracy	7.75E-05	5.91E-06

TABLE VI
COMPARISON OF OPTIMIZATION MODELS—TEST SYSTEM B

Index	NLP method	Diagonalization method
Number of variables per problem	4281	426
Number of constraints per problem	2611	430
Total CPU seconds	727	180
Total solver iterations	1348	3450
Accuracy	6.55E-05	1.26E-07

computational requirements for Test system A. Three sweeps of the diagonalization method were needed to solve the problem where two MPECs are solved in each sweep. Each MPEC problem takes 30 solver iterations and 0.185 s to solve, on average. The last row of Table V shows the solution accuracy. In the case of the NLP approach, this index denotes the value of C_{pen} in (55), and is Δ_{tol} in the case of the diagonalization method.

Likewise, the solutions of the two optimization problems were compared for Test system B. In this case, too, solutions are very close and differences are negligible. Table VI compares the performance of the two optimization methods. Notice the large problem size and computing time in the case of the NLP approach. The solution time can be reduced using a good starting point. (We used a flat-start setup with zero slack variables.) The other factor affecting the solution time is the convergence tolerance of the solver algorithm. The figures reported in Table VI correspond to a convergence tolerance of 1.0E-6. When this valued is reduced to 1.0E-4, the CPU seconds and the number of iterations would become 283 and 1257, respectively. This means the solution time can be reduced to half of the value presented in Table VI without significant changes in the optimization results.

In the case of the diagonalization method, four sweeps are needed to find the solution. Each sweep solves five MPECs where each MPEC problem takes 173 iterations and 1.04 s, on average. Although the diagonalization methods can solve the problem faster, in some cases it does not converge even after a large number of iterations. This can happen when security limits become binding. It is to be noted that in some cases the initial sweeps may converge to infeasible points, but the optimal solution is eventually achieved at a larger number of sweeps.

B. Heuristic Tests

A number of factors can affect the solvability of the proposed nonconvex EPEC model including starting points. Aiming at verifying the effect of starting points, we created 120 sets of uniformly distributed random starting points. They were so generated to be logical with the problem constraints. The EPEC problems were then solved for each set of starting points. Assuming the base case scenarios, we applied this procedure to Test systems A and B. In the case of Test system A, 109 problems out of these 120 problems were solved and converged to the solution presented in Section III, and the rest converged to infeasible points. In the case of Test system B, 89 problems were solved and converged to the same solution found in the previous runs (see Section III).

The other heuristic test that was implemented to check the existence of multiple equilibria is as follows. We introduced an additional constraint in the form of $f_v \leq f_v^*$ to the MPEC problem (29)–(36), which incorporates new bounds for the objective function. In this constraint, f_v denotes the objective function (29) and f_v^* is the optimal value found in the previous runs. The new MPEC problems with the additional constraints are then solved to check the existence of equilibria with lower f_v^* values. We applied this ex-pot test to both test systems assuming only the base case scenarios.

The problems became infeasible when the bound on the new constraint was reduced to values less than the optimal value determined in the previous runs. Thus, the solution did not improve using this technique. Results from these ex-post heuristic tests, too, indicate that the solution presented in Section III denote optimal equilibria.

C. Modeling Features

Figures reported in Tables V and VI indicate that different formulations give rise to problems of differing size. The problem size in the NLP approach significantly increases with the number of discos due to additional (slack) variables required for dealing with the complementarity conditions. Moreover, since each disco assigns a unique set of dual multipliers to the KKT constraints of the lower-level problem, the number of these variables will also increase with the number of discos. The benefit of the NLP approach is that the resulting EPEC model can be solved by a single optimization problem using standard NLP solvers. Moreover, the NLP approach can detect situations where the EPEC problem has no solution [11]. On the other hand, the problem size in the diagonalization method is smaller and the optimization problem is computationally tractable because only one MPEC is solved at a time. However, the diagonalization method may not converge when cycling occurs [26]. The advantage of the diagonalization method is its conceptual simplicity and that it does not require the gradient of the problem to be computed which can be a lengthy error-prone process, especially when extensive level of modeling details are considered. For instance, if the disco includes the IL benefit into its objective, which comes from the difference between the ISO price for the IL and the fixed price that the disco pays customers, this can complicate the resulting EPEC problem for large distribution networks with numerous IL offering customers. In such cases the problem can be solved more efficiently by the diagonalization method.

The NLP model and the diagonalization method were implemented in AMPL and solved using the IPOPT solver [30]. All

simulations were carried out on a Windows-based laptop computer clocking at 1.8 GHz with 2 GB of RAM.

V. Conclusion

The operational decision making of a disco in a competitive environment was formulated as a bilevel optimization problem. The impacts of rival strategies on the disco decision was incorporated in the decision making process of the disco. This resulted in a multi-disco EPEC game problem which was reformulated as a single nonlinear optimization problem and solved by a standard NLP solver. The optimality of the solution was also examined using three different methodologies including an alternative MPEC formulation and two ex-post heuristic tests.

While most equilibrium models are based on linear dc models of power system or neglect the distribution side competition, a security-constraints ac OPF model was developed wherein various components of the distribution and transmission systems are modeled. The proposed approach can accurately account for the impacts of DG and IL on the voltage and reactive flow of the distribution system and provide nodal prices both at the transmission and distribution levels for payment calculations.

The application of the proposed model was illustrated using two test systems and numerous case studies. It was shown that discos can reduce operating costs and feeder losses using IL option and DG resources while interacting with the wholesale market and the other competitors.

Appendix A

Reference [12] employs a rectangular coordinate for developing an EPEC model. In this coordinate bus voltages and nodal power injections are expressed as follows:

$$V_i = e_i + jf_i \tag{A1}$$

$$e_i = V_i \cos\theta_i, \quad f_i = V_i \sin\theta_i \tag{A2}$$

$$V_i^2 = e_i^2 + f_i^2, \quad \theta_i = \tan^{-1}\left(\frac{f_i}{e_i}\right) \tag{A3}$$

$$P_i = \sum_j \{e_i (G_{ij}e_j - B_{ij}f_j) + f_i (B_{ij}e_j + G_{ij}f_j)\} \tag{A4}$$

$$Q_i = \sum_j \{f_i (G_{ij}e_j - B_{ij}f_j) - e_i (B_{ij}e_j + G_{ij}f_j)\} \tag{A5}$$

where B_{ij} represents element ij of suseptance matrix, and G_{ij} is element ij of conductance matrix.

Appendix B

Tables VII–XII present the data of the ISO and disco systems used in Test system A.

TABLE VII
Generator Data—Test System A

	Node	
	1	6
$a_{Pg,u,i}$ ($/MW^{2}h)	0.006	0.006
$b_{Pg,u,i}$ ($/MWh)	105	90
$a_{Qg,u,i}$ ($/MVar^{2}h)	0.0006	0.0006
$a_{Qg,u,i}$ ($/MVarh)	10.5	9.0
$\overline{P}$ (MW)	30	30
$[\underline{Q}, \overline{Q}]$ (MVar)	[-10, 20]	[-10, 20]

TABLE VIII
Line Data of the ISO Grid—Test System

#	From	To	R (pu)	X (pu)	B (pu)	$\overline{S}$ (MVA)
1	1	2	0.0194	0.0592	0.0052	0.2
2	1	3	0.0540	0.2230	0.0197	0.3
3	1	6	0.0581	0.1763	0.0150	0.3
4	2	3	0.0388	0.1183	0.0105	0.15
5	3	4	0.0872	0.2645	0.0224	0.25
6	4	5	0.0279	0.0852	0.0075	0.15
7	4	6	0.0697	0.2116	0.0180	0.4
8	5	6	0.0252	0.0769	0.0068	0.3

TABLE IX
DG Units Data—Test System A

v	Bus	$a_{dg,v,n}$ ($/MW^{2}h)	$b_{dg,v,n}$ ($/MWh)	$\overline{P}$ (MW)	$[\underline{Q}, \overline{Q}]$ (Mvar)
1	6	0.002	25	10	[-1.67, 3.33]
2	6	0.002	25	10	[-1.67, 3.33]

TABLE X
Load Data of Disco 1–Test System A

Node	$P_{L,v,n}$ (MW)	$Q_{L,v,n}$ (Mvar)	$a_{IL,v,n}$ ($/MW^{2}h)	$a_{IL,v,n}$ ($/MWh)
2	1.5	0.75	0.0065	100
3	2.5	1.25	0.0080	90
4	3.0	1.5	0.0065	105
5	1.5	0.75	0.0060	80
6	0.75	0.375		

TABLE XI
Load Data of Disco 2–Test System A

Node	$P_{L,v,n}$ (MW)	$Q_{L,v,n}$ (Mvar)	$a_{IL,v,n}$ ($/MW^{2}h)	$a_{IL,v,n}$ ($/MWh)
2	1.5	0.75	0.0065	100
3	2.5	1.25	0.0080	90
4	3.0	1.5	0.0065	105
5	1.5	0.75	0.0060	80
6	0.75	0.375		

TABLE XII
Line Data of Discos 1,2–Test System A

#	From	To	R (pu)	X (pu)	$\overline{S}$ (MVA)
1	1	2	0.7283	0.8509	14
2	1	3	0.3100	0.3623	14
3	2	4	0.248	0.2898	14
4	3	5	0.3100	0.3623	14

References

[1] D. Kirschen and G. Strbac, *Fundamentals of Power System Economics*. New York: Wiley, 2004.

[2] D. T. Nguyen and M. D. Groot, "Pool-based demand response exchange-concept and modeling," *IEEE Trans. Power Syst.*, vol. 26, no. 3, pp. 1777–16, Aug. 2011.
[3] A. Algarni and K. Bhattacharya, "A generic operations framework for discos in retail electricity markets," *IEEE Trans. Power Syst.*, vol. 24, no. 1, pp. 356–367, Feb. 2009.
[4] R. Palma-Behnke, J. L. A. Cerda, L. Vargas, and A. Jofre, "A distribution company energy acquisition market model with the integration of distribution generation and load curtailment options," *IEEE Trans. Power Syst.*, vol. 20, no. 4, pp. 1718–1727, Nov. 2005.
[5] A. Jiménez-Estévez, R. Palma-Behnke, R. Torres-Avila, and L. S. Vargas, "A competitive market integration model for distributed generation Guillermo," *IEEE Trans. Power Syst.*, vol. 22, no. 4, pp. 2161–2169, Nov. 2007.
[6] H. Li, Y. Li, and Z. Li, "A multi-period energy acquisition model for a distribution company with distributed generation and interruptible load," *IEEE Trans. Power Syst.*, vol. 22, no. 2, pp. 588–596, May 2007.
[7] J.-S. Pang and M. Fukushima, Quasi-Variational Inequalities, Generalized Nash Equilibria, and Multi-Leader-Follower Games, Johns Hopkins Univ., Baltimore, MD, Tech. Rep., 2002.
[8] M. Latorre and S. Granville, "The Stacklberg equilibrium applied to ac power system—A noninterior point algorithm," *IEEE Trans. Power Syst.*, vol. 18, no. 2, pp. 611–618, May 2003.
[9] B. H. Hobbs, C. B. Metzler, and J.-H. Pang, "Strategy gaming analysis for electric power systems: An MPEC approach," *IEEE Trans. Power Syst.*, vol. 15, no. 2, pp. 638–645, May 2000.
[10] H. Haghighat, H. Seifi, and A. R. Kian, "Gaming analysis in joint energy and spinning reserve markets," *IEEE Trans. Power Syst.*, vol. 22, no. 4, pp. 2074–2085, Nov. 2007.
[11] S. Leyffer and T. Munson, "Solving multi-leader-common-follower games," *Optimiz. Meth. Softw.*, vol. 25, no. 4, pp. 601–623, Aug. 2010.
[12] G. Bautista, M. F. Anjos, and A. Vannelli, "Formulation of oligopolistic competition in ac power networks: An NLP approach," *IEEE Trans. Power Syst.*, vol. 22, no. 1, pp. 105–116, Feb. 2007.
[13] G. Bautista, M. F. Anjos, and A. Vannelli, "Numerical study of affine supply function equilibrium in ac network-constrained markets," *IEEE Trans. Power Syst.*, vol. 22, no. 3, pp. 1174–1185, Aug. 2007.
[14] X. Wang, Y. Li, and S. Zhang, "Oligopolistic equilibrium analysis for electricity markets: A nonlinear complementarity approach," *IEEE Trans. Power Syst.*, vol. 19, no. 3, pp. 1348–1355, Aug. 2004.
[15] J. M. López-Lezama, A. Padilha-Feltrin, J. Contreras, and J. I. Muñoz, "Optimal contract pricing of distributed generation in distribution networks," *IEEE Trans. Power Syst.*, vol. 26, no. 1, pp. 128–136, Feb. 2011.
[16] H. Haghighat, C. Canizares, and K. Bhattacharya, "Dispatching reactive power considering all providers in competitive electricity markets," in *Proc. IEEE PES General Meeting*, 2010.
[17] N. H. Dandachi, M. J. Rawlins, O. Alsac, M. Paris, and B. Stott, "OPF for reactive pricing studies on the NGC system," *IEEE Trans. Power Syst.*, vol. 11, no. 1, pp. 226–232, Feb. 1996.
[18] K. Xie, Y. H. Song, J. Stonham, E. Yu, and G. Liu, "Decomposition model and interior point methods for optimal spot pricing of electricity in deregulation environments," *IEEE Trans. Power Syst.*, vol. 15, no. 1, pp. 39–50, Feb. 2000.
[19] J. B. Gil, T. G. roman, J. J. Rios, and P. S. Martin, "Reactive power pricing: A conceptual framework for remuneration and charging procedure," *IEEE Trans. Power Syst.*, vol. 15, no. 2, pp. 483–489, May 2000.
[20] Federal Energy Regulatory Commission (FERC). 2005. Principles for Efficient and Reliable Reactive Power Supply and Consumption. Staff Report. Docket No. AD05–1-000. Washington, DC, Feb. 4. [Online]. Available: http://www.ferc.gov.
[21] R. J. Thomas, T. D. Mount, R. Schuler, W. Schulze, R. Zimmerman, F. Alvarado, B. C. Lesieutre, P. N. Overholt, and J. H. Eto, "Efficient and reliable reactive-power supply and consumption: Insights from an integrated program of engineering and economic research," *Electr. J.*, vol. 21, no. 1, pp. 70–81, 2008.
[22] M. Braun, "Reactive power supply by distributed generators," in *Proc. IEEE PES General Meeting*, Pittsburgh, PA, Jul. 20–24, 2008.
[23] P. Sotkiewicz and J. M. Vignolo, "Nodal pricing for distribution networks: Efficient pricing for efficiency enhancing DG," *IEEE Trans. Power Syst.*, vol. 21, no. 2, pp. 1013–1014, May 2006.
[24] P. Sotkiewicz and J. M. Vignolo, "Towards a cost causation-based tariff for distribution networks with DG," *IEEE Trans. Power Syst.*, vol. 22, no. 3, pp. 1051–1060, Aug. 2007.
[25] P. M. De oliveira De-Jesús, M. T. Ponce de Leão, J. M. Yusta, H. M. Khodr, and A. J. Urdaneta, "Uniform marginal pricing for the remuneration of distribution networks," *IEEE Trans. Power Syst.*, vol. 20, no. 3, pp. 1302–1310, Aug. 2005.
[26] C.-L. Su, A Sequential NCP Algorithm for Solving Equilibrium Problems With Equilibrium Constraints, Department of Management Science and Engineering, Stanford Univ., 2004.
[27] J. Zhao, B. Brereton, and M. Montalvo, "Gaming-based reserve constraints penalty factor," *IEEE Trans. Power Syst.*, vol. 26, no. 2, pp. 616–626, May 2011.
[28] é Melo, E. M. Almeida Neves, and L. H. A. Pazzini, "The Brazilian electricity model: An overview of the current structure and market design," in *Proc. IEEE 8th Int. Conf. European Energy Market (EEM)*, Zagreb, Croatia, May 2011.
[29] D. Doeh, C. Wood, A. Popov, S. Fomínykh, and N. Mouratova, Reform of the Russian Electricity Industry, EBRD Law Institute, 2008. [Online]. Available: http://www.ebrd.com/pubs/.
[30] R. Fourer, D. M. Gay, and B. W. Kernighan, *AMPL: A Modeling Language for Mathematical Programming*. Pacific Grove, CA: Duxbury, 2002.

Hossein Haghighat (M'08) received the Ph.D. degree in electrical engineering from Tarbiat Modares University, Tehran, Iran, in 2007.

His research interests include electricity market operation and optimization.

Scott W. Kennedy (M'08) received the Ph.D. degree in engineering sciences and the S.M. degree in applied math from Harvard University, Cambridge, MA, in 2003.

He is an Associate Professor at the Masdar Institute of Science and Technology, Abu Dhabi, UAE. His current research interests include the integration of renewable energy sources into power networks, with an emphasis on the interactions between power markets and power system.